Journal of Applied Polymer Science

Influence of processing conditions on polymorphic behavior, crystallinity, and morphology of electrospun poly(vinylidene fluoride) nanofibers

Maedeh Baqeri,[1] Mohammad Mahdi Abolhasani,[2] Mohammad Reza Mozdianfard,[1,2] Qipeng Guo,[3] Azam Oroumei,[3] Minoo Naebe[3]

[1]Institute of Nanoscience and Nanotechnology, University of Kashan, Kashan, Iran
[2]Department of Chemical Engineering, University of Kashan, Kashan, Iran
[3]Institute for Frontier Materials, Deakin University, Victoria 3216, Australia
Correspondence to: M. M. Abolhasani (E-mail: abolhasani@kashanu.ac.ir)

ABSTRACT: The polymorphism and crystallinity of poly(vinylidene fluoride) (PVDF) membranes, made from electrospinning of the PVDF in pure *N*,*N*-dimethylformamide (DMF) and DMF/acetone mixture solutions are studied. Influence of the processing and solution parameters such as flow rate, applied voltage, solvent system, and mixture ratio, on nanofiber morphology, total crystallinity, and crystal phase content of the nanofibers are investigated using scanning electron microscopy, wide-angle X-ray scattering, differential scanning calorimetric, and Fourier transform infrared spectroscopy. The results show that solutions of 20% w/w PVDF in two solvent systems of DMF and DMF/acetone (with volume ratios of 3/1 and 1/1) are electrospinnable; however, using DMF/acetone volume ratio of 1/3 led to blockage of the needle and spinning process was stopped. Very high fraction of β-phase (~79%–85%) was obtained for investigated nanofiber, while degree of crystallinity increased to 59% which is quite high due to the strong influence of electrospinning on ordering the microstructure. Interestingly, ultrafine fibers with the diameter of 12 and 15 nm were obtained in this work. Uniform and bead free nanofiber was formed when a certain amount of acetone was added in to the electrospinning solution. © 2015 Wiley Periodicals, Inc. J. Appl. Polym. Sci. **2015**, *132*, 42304.

KEYWORDS: crystallization; electrospinning; morphology; nanostructured polymers; properties and characterization

Received 12 January 2015; accepted 5 April 2015
DOI: 10.1002/app.42304

INTRODUCTION

Poly(vinylidene fluoride) (PVDF) is one of the semicrystalline thermoplastic polymers that has attracted many interests due to its excellent mechanical properties, chemical stability, and outstanding electrical properties.[1–8] PVDF has been found to have a strong piezo, pyro, and ferroelectric property[9–11] its piezoelectric coefficient is almost 10 times larger than other polymers. Another interesting feature of PVDF is its structural polymorphism. Being a semicrystalline polymer with a typical crystallinity of 50%, and with a molecular structure consists of the repeated monomer unit $(-CH_2CF_2-)_n$,[12] PVDF can demonstrate several crystalline phases. Depending on the chain conformations (namely trans (T) or gauche (G) linkages), PVDF shows five crystalline phases: non-polar α-phase and ε-phase, as well as polar β-phase, δ-phase, and γ-phase.[4,5,13–16]

Among all crystalline phases, the most investigated PVDF phases are α-, β-, and γ-phases. This is mainly due to the superior characteristics of PVDF as a result of the presence of these phases. The all trans, TTT, planar zigzag configurations confers to the β-phase, leads to the highest permanent dipole which improves piezoelectric and pyroelectric properties.[17,18] In order to obtain the β-phase PVDF, electrical poling and mechanical stretching processes are required during the manufacturing process to align the dipoles in the crystalline PVDF structures.[19,20]

Due to the development of the field of nanotechnology over the last decades, there has been an escalated increasing in electrospinning. Electrospinning is a fairly simple and inexpensive technique that can produce fibers in nanoscales.[21–25] Such nanofibers may then be used for a variety of different applications, such as nanocatalysis, tissue scaffolds, protective clothing, filtration, and optical electronics.[26–28] When the diameter of polymer fiber materials decreases from micrometers to submicrons or nanometers, there appear several interesting characteristics such as very large surface area to volume ratio, flexibility in surface functionalities, and superior mechanical performance compared to any other known form of the materials.[29,30]

Nanofibers represent one of the most important one-dimensional (1D) nanostructures standing at the leading edge of nanoscience and nanotechnology.[31] In electrospinning, an electric field is applied to a polymer solution to produce polymeric fibers onto a target collector.[32–34] In this process, fibers are formed when the applied electric field overcomes the surface tension of the droplet, and a charged jet of polymer solution is ejected from the capillary tip. The jet extends towards the target attached to the ground and solidifies on it.[35,36] Recent advances in the electrospinning process provide the possibility of in situ mechanical stretching and electric poling to obtain ferroelectric β-PVDF from its polymer solution.[37,38]

Processing conditions of PVDF significantly affect the microstructure, β-phase content, and degree of crystallinity of the resulting nanofiber. In general, electrospinning has been found to strongly influence the formation of crystalline phases in polymer nanofibers.[21–25] It has been reported that β-phase formation in PVDF electrospun nanofibers is higher than that of PVDF cast films.[39,40]

Electrospinning conditions, namely solution parameters, processing, and environmental conditions strongly affect the fiber morphology as well as the phase in which PVDF crystallizes.

Zheng *et al.*[41] reported that fast evaporation of the solvent favor the development of β polymorph, high voltage or high stretching ratio of the jets also result formation in β polymorph. Orientation of the electrospun fibers using a rotating collector also favored crystallization of β polymorph.[42]

Whilst there are several reports on influence of processing conditions on nanofiber properties, to the best of our knowledge the effects of processing conditions on formation of different polymorphs in PVDF nanofibers has not been comprehensively studied. Furthermore, less attention has been paid to quantitative analysis of different polymorphs formation. In this work, we present a study of the influence of the electrospinning process parameters (applied voltage and flow rate), and solution parameters (solvent type and mixture ratio) on the fiber morphology, distribution of fiber diameters, fraction of β-phase, and the crystallinity of PVDF electrospun nanofibers.

EXPERIMENTAL

Materials

PVDF (Solef1010) with molecular weight of 1×10^5 g/mol was supplied by Solvay, Belgium. Dimethylformamide (DMF) and acetone were obtained from Merck, Germany.

Sample Preparation

Three polymer solutions were prepared using 20% PVDF dissolved in DMF and in 3 : 1 and 1 : 1 (by weight) DMF/acetone mixed solutions, respectively. Polymer solutions were stirred for 24 h at 70°C.

The prepared polymer solutions were then placed in a 5 mL plastic syringe fitted with a steel needle (0.75 mm diameter). Electrospinning (Nano Azma, Iran, apparatus) was conducted under 13 and 21 kV using a high voltage power supply. A syringe pump was used to feed the polymer solutions into the needle tip at the rates of 0.5 and 1 mL/h. The electrospun fibers were collected on a rotating drum that was placed 17 cm away from the needle. The rotation speed of drum was 2500 rpm. PVDF concentration and travelling distance from the needle to the collector were kept fixed. Information on PVDF electrospun nanofibers are presented in Table I.

Table I. Solvent, Voltage, and Flow Rate Used to Prepare Electrospun[a] Nanofibers

Sample code	DMF/acetone	Voltage (kV)	Flow rate (mL/h)
RE-1	1/0	13	0.5
RE-2	1/0	13	1
RE-3	1/0	21	0.5
RE-4	1/0	21	1
TE-1	3/1	13	0.5
TE-2	3/1	13	1
TE-3	3/1	21	0.5
TE-4	3/1	21	1
SE-1	1/1	13	0.5
SE-2	1/1	13	1
SE-3	1/1	21	0.5
SE-4	1/1	21	1

[a] Samples were electrospun from 20 wt % PVDF polymer solution.

Characterizations Techniques

Differential scanning calorimetry (DSC) was conducted using a TA Instrument Q200. Samples were heated from room temperature to 210°C at a rate of 10°C/min.

Fourier transform infrared spectroscopy (FTIR) was performed to study different polymorphs of the samples using Bruker 70 equipped with ATR unit. For each sample, 64 scans between 500 cm^{-1} and 1500 cm^{-1} with a resolution of 4 cm^{-1} were collected.

Scanning electron microscopy (SEM) was performed using Zeiss SupraTM 55VP electron microscope. Samples were sputter-coated with a thin layer of gold before imaging. Fiber diameter distribution was calculated using microstructure measurement software and on the basis of SEM images.

Two-dimensional (2D) WAXD analysis were performed using an imaging plate equipped with an 18 kW X-ray rotating anode generator (Cu Ka radiation, 1.54 A°, Rigaku automated X-ray imaging system with 1500 × 1500 pixel resolution). The air scattering was subtracted from the WAXD patterns. These tests were all performed at ambient conditions.

RESULTS AND DISCUSSION

Polymer solution characteristics play a major role in governing the morphology and properties of the electrospun fibers. Among them, solvent parameters such as dielectric constant, volatility, and boiling point as well as solution parameters of concentration and the polymer molecular weight are considered as the most effective ones. Flow rate, applied voltage, temperature, spinning distance, and needle diameter are the main process parameters controlling the jet formation and solvent evaporation. Although all the aforementioned factors can indirectly affect the fiber diameter and orientation, the collection

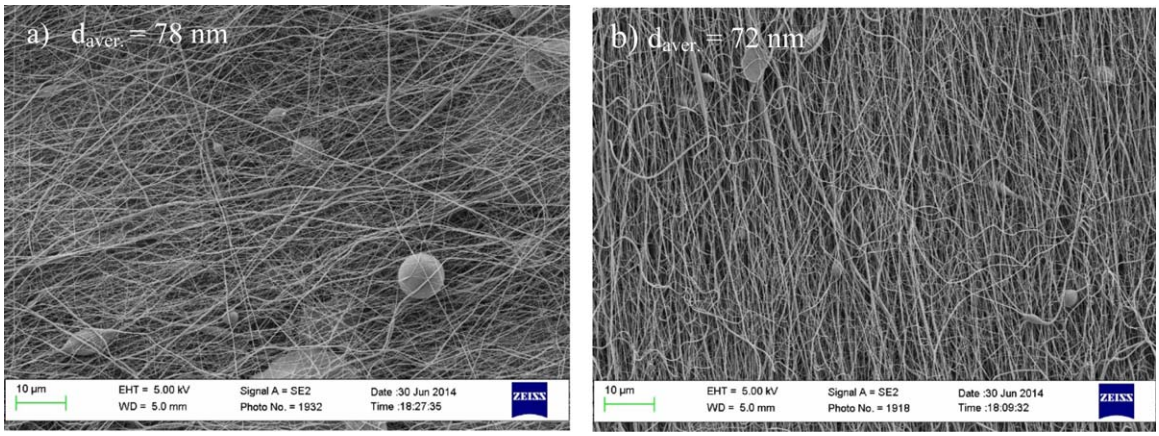

Figure 1. SEM images of electrospun PVDF nanofibers at spinning distance of 17 cm, flow rate 1 mL/h, and voltage of (a) 13 kV and (b) 21 kV (code RE-2 and RE-4 samples). [Color figure can be viewed in the online issue, which is available at wileyonlinelibrary.com.]

procedure (namely a static or rotating drum and the rotating drum speed) has the most effective role on the fiber morphology.[17,18] Consequently, the numbers of parameters that influence the morphological and crystalline properties are quite high; therefore, in each step only one parameter was changed while others kept constant. Solutions with 20% PVDF in DMF and DMF/acetone solvents were successfully electrospun on aluminized rotating collector. Electrospun nanofibers were prepared and the influence of applied voltage, flow rate, and solvent ratio on the nanofiber characteristics in terms of fiber diameter, morphology, crystallinity, and polymorphism were investigated.

Influence of Applied Voltage

Morphological Properties. The influence of applied voltage was investigated where keeping a constant flow rate of 0.5 and 1 mL/h, and spinning distance 17 cm. Figure 1(a,b) shows the SEM images of electrospun PVDF membranes prepared at 13 and 21 KV, respectively.

As seen in Figure 1, increasing the voltage from 13 to 21 kV in samples obtained from DMF as solvent (sample RE), results in smaller beads. Nevertheless, as is seen in Figure 2, by addition of acetone to pure DMF, more beads are formed in electrospun fibers. Given the constant polymer concentration, it was found that there is a greater tendency for beads formation at a higher voltage.

Figure 3 illustrates the effect of applied voltage on the distribution of fiber diameters in two sample categories. As a result of applying higher voltage, the diameter of the fibers is decreased in most samples. Broader distribution of the fiber diameters is seen at lower applied voltage in several samples [Figure 3(b)]. As the changes in the applied voltage could also affect other parameters such as the traveling time of the jet which has an opposite effect on the fiber diameter, thus in some samples it is relatively hard to distinguish the effects of applied voltage. In the electrospinning method, stretching and acceleration of the polymer jet in high electric field results in the formation of the fine fibers. Increase in applied voltage would increase the jet velocity by inducing a higher charge density on the surface of the ejected jet. This phenomenon imposes higher elongation force to the jet. Therefore, it can be concluded that the diameter of the final fibers will decrease by increasing of applied voltage.

However, an increase in the applied voltage also enhances the degree of instability of the polymer jets at the same time, which results in formation of nanofibers with more beads. Therefore, the higher voltage could produce finer as well as more beaded fibers.

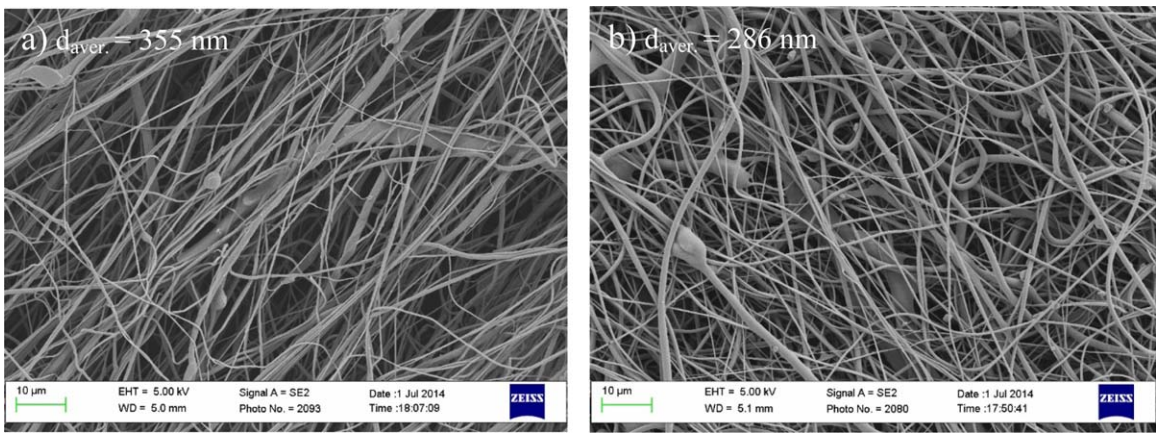

Figure 2. Morphology of electrospun PVDF nanofibers at traveling distance of 17 cm, flow rate 1 mL/h, and voltage of (a) 13 kV and (b) 21 kV (code SE-2 and SE-4 samples). [Color figure can be viewed in the online issue, which is available at wileyonlinelibrary.com.]

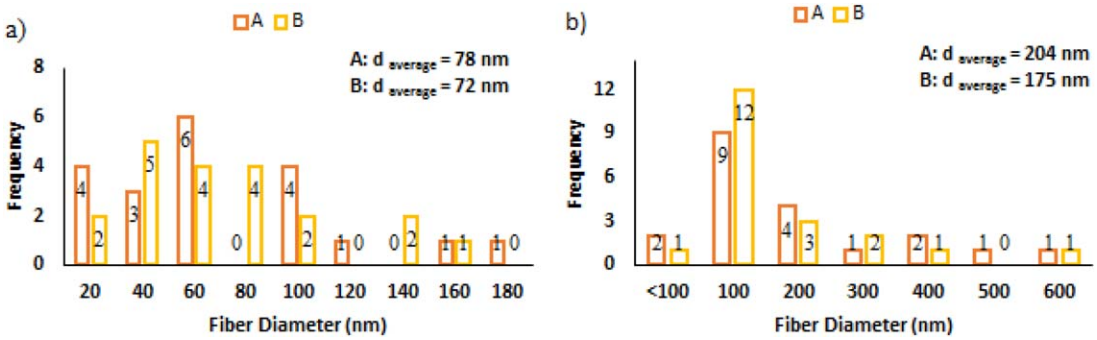

Figure 3. Diameter distribution of electrospun PVDF nanofibers at spinning distance of 17 cm, flow rate 1 mL/h, and voltage of (A) 13 kV and (B) 21 kV ((a) code RE samples and (b) code TE samples). [Color figure can be viewed in the online issue, which is available at wileyonlinelibrary.com.]

Polymorphism and Crystallinity. High voltage not only affects the fiber diameter but also can influence the crystallinity of the fibers.[43] Effects of the voltage on different polymorph formation were characterized by FTIR spectroscopy. The relative content of α and β polymorphs were calculated by eq. (1):[44]

$$F(\beta)=\frac{X_\beta}{X_\alpha+X_\beta}=\frac{A_\beta}{1.26A_\alpha+A_\beta} \quad (1)$$

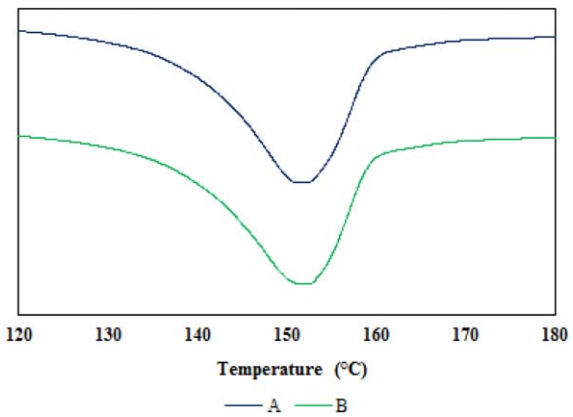

Figure 4. DSC thermograms for the electrospun PVDF nanofibers obtained from electrospinning at the flow rate of 1 mL/h and different applied voltages (A) 13 kV and (B) 21 kV (code SE-2 and SE-4 samples). [Color figure can be viewed in the online issue, which is available at wileyonlinelibrary.com.]

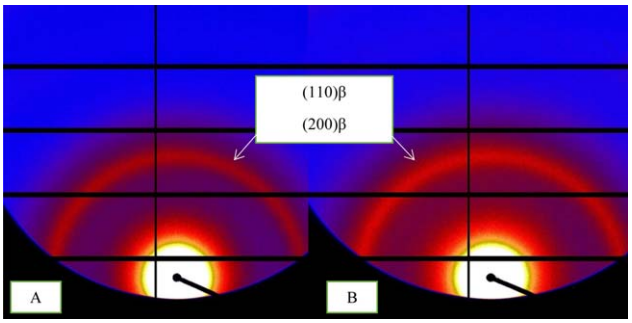

Figure 5. 2D WAXD images of electrospun PVDF nanofibers at traveling distance of 17 cm, flow rate 1 mL/h, and voltage of (A) 13 kV and (B) 21 kV (code RE-2 and RE-4 samples). [Color figure can be viewed in the online issue, which is available at wileyonlinelibrary.com.]

where X_α and X_β are crystalline mass fractions of α- and β-phases respectively, and A_α and A_β are their corresponding absorption bands at 763 and 840 cm^{-1}.[45] The degree of crystallinity (ΔX_c) of each sample was determined from the DSC curves using eq. (2):

$$\Delta X_c=\frac{\Delta H}{x_\alpha\Delta H_\alpha+x_\beta\Delta H_\beta} \quad (2)$$

where ΔH is the melting enthalpy of the sample under consideration, ΔH_α and ΔH_β are the melting enthalpies of a 100% crystalline sample in the α- and β-phases, respectively, and x_α and x_β are the amount of the α- and β-phases in the sample, respectively.[46] In this study, a value of 93.07 J g^{-1} and 103.4 J g^{-1}[46]

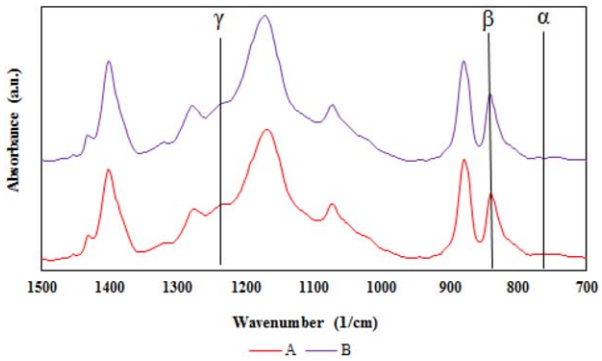

Figure 6. Normalized FTIR spectra of electrospun PVDF nanofibers at traveling distance of 17 cm, flow rate 1 mL/h, and voltage of (A) 13 kV and (B) 21 kV (code RE-2 and RE-4 samples). Curves are shifted vertically for clarity. [Color figure can be viewed in the online issue, which is available at wileyonlinelibrary.com.]

Table II. Fraction of β-Phase $F(\beta)$ (and Total Crystallinity) of the Electrospun PVDF Nanofibers Calculated from DSC Measurements

Sample RE	$F(\beta)$ (voltage = 13 kV)	$F(\beta)$ (voltage = 21 kV)
Flow rate = 0.5 mL/h	0.80 (X_{total} = 0.53)	0.83 (X_{total} = 0.55)
Flow rate = 1 mL/h	0.79 (X_{total} = 0.59)	0.82 (X_{total} = 0.49)

Table III. Fraction of β-Phase $F(\beta)$ (and Total Crystallinity) of the PVDF Nanofibers by Electrospinning

Sample TE	$F(\beta)$ (voltage = 13 kV)	$F(\beta)$ (voltage = 21 kV)
Flow rate = 0.5 mL/h	0.83 (X_{total} = 0.41)	0.84 (X_{total} = 0.49)
Flow rate = 1 mL/h	0.84 (X_{total} = 0.45)	0.81 (X_{total} = 0.54)

Table IV. Fraction of β-Phase $F(\beta)$ (and Total Crystallinity) of the PVDF Nanofibers by Electrospinning

Sample SE	$F(\beta)$ (voltage = 13 kV)	$F(\beta)$ (voltage = 21 kV)
Flow rate = 0.5 mL/h	0.84 (X_{total} = 0.42)	0.83 (X_{total} = 0.42)
Flow rate = 1 mL/h	0.82 (X_{total} = 0.47)	0.82 (X_{total} = 0.46)

was used for the ΔH_α and ΔH_β, respectively, and x_α and x_β were obtained from the FTIR measurements based on eqs. (3–5):

$$A_{762} = K_\alpha^{762} X_\alpha t \quad (3)$$

$$A_{1275} = K_\beta^{1275} X_\beta t \quad (4)$$

$$A_{835} = (K_\beta^{835} X_\beta + K_\gamma^{835} X_\gamma + K_{am}^{835} (1 - X_{total}))t \quad (5)$$

where A_j is the baseline-corrected absorbance in J cm^{-1}, K_i^j is the absorption coefficient at J cm^{-1} for the i-phase, X_i is the mole fraction of the i-phase, X_{total} is the total crystallinity, and t is the thickness in micrometers. The thickness of the nanofibers film was calculated from the IR absorption band at 1070 cm^{-1}, in which the absorption coefficient is independent from the crystalline phase of the polymer, and corresponds to: $A_{1070} = 0.095t + 0.07$.[27] The values obtained for the absorption coefficients were 0.0259, 0.365, 0.150, 0.140, and 0.132 μm^{-1}, for K_{am}^{835}, K_α^{762}, K_γ^{835}, K_β^{1275}, and K_β^{835}, respectively.[44] Figure 4 shows DSC curves for PVDF nanofiber samples.

The DSC measurements provides the heat of fusion (ΔH), as well as the total crystallinity (X_{total}) of PVDF samples. The ΔH value was calculated using the area under the peak in the DSC curves. The 2D WAXD data provides useful information on the polymorphism structure of the nanofibers. Figure 5 shows the WAXD patterns of two electrospun nanofibers obtained from different voltages. Diffraction arcs related to β polymorph can be observed in both patterns as pointed by arrows.

The FTIR spectra of the RE samples at different applied voltage are shown in Figure 6. As is seen, β polymorph characteristic peak is clearly seen at 840 cm^{-1} while α and γ peaks are absent. FTIR result confirms the obtained WAXD data discussed above.

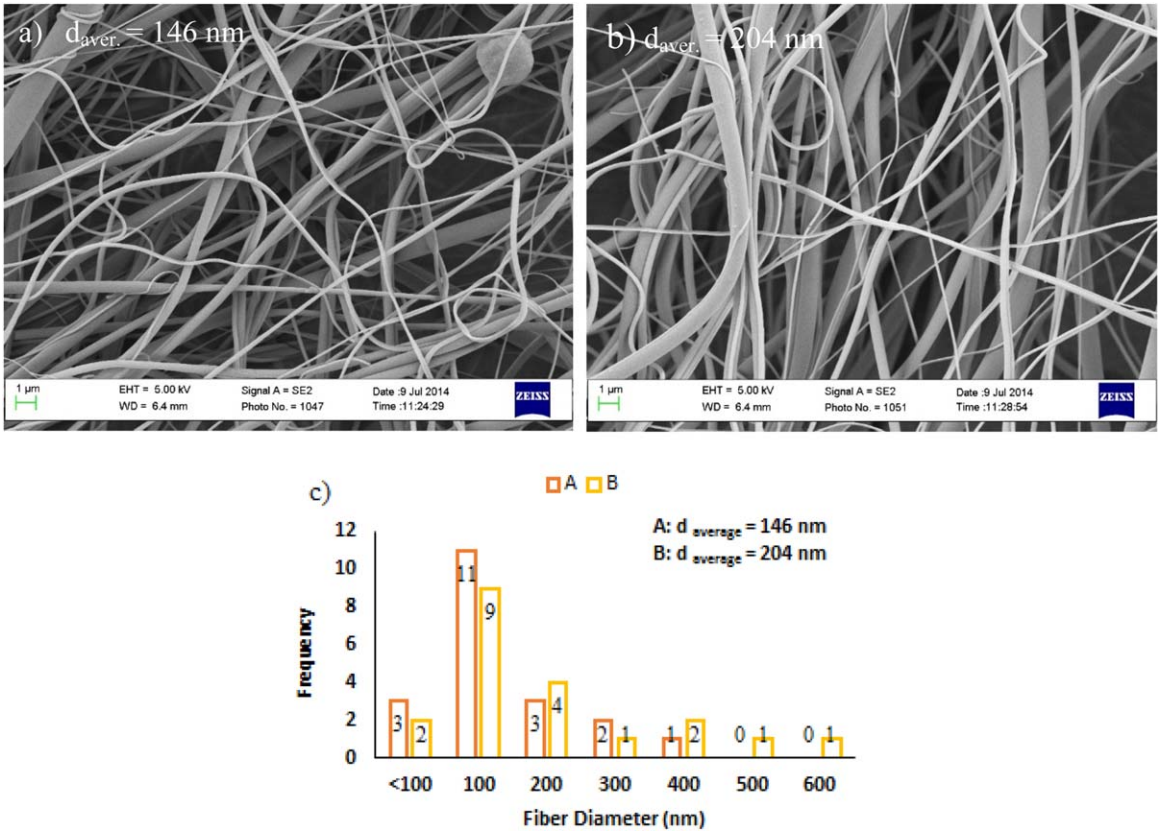

Figure 7. Morphology and diameter distribution of electrospun PVDF nanofibers at spinning distance of 17 cm, voltage 13 kV, and flow rate of (A) 0.5 and (B) 1 mL/h (code TE-1 and TE-2 samples). [Color figure can be viewed in the online issue, which is available at wileyonlinelibrary.com.]

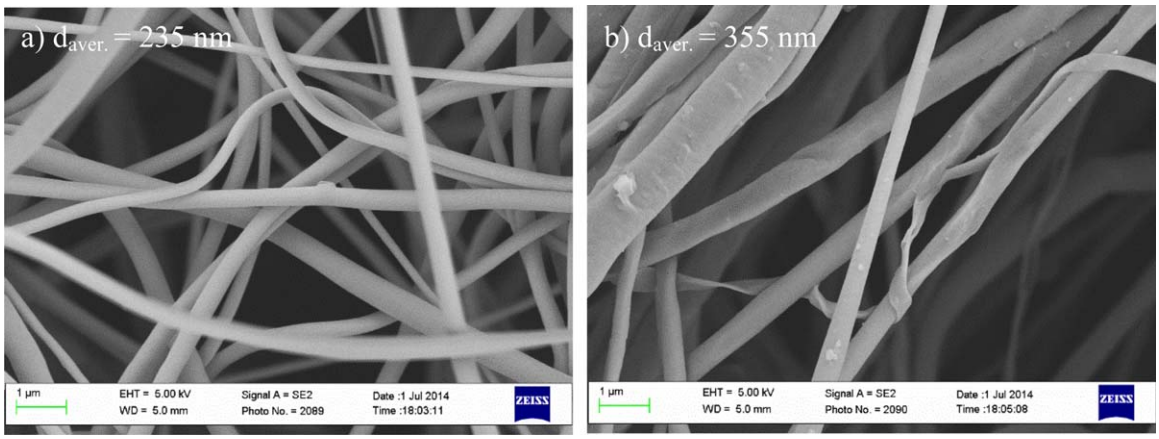

Figure 8. Morphology and diameter distribution of electrospun PVDF nanofibers at spinning distance of 17 cm, voltage 13 kV, and flow rate of (a) 0.5 (d_{av} = 235 nm) and (b) 1 mL/h (d_{av} = 355 nm) (code SE-1 and SE-2 samples). [Color figure can be viewed in the online issue, which is available at wileyonlinelibrary.com.]

The effect of electrospinning processing parameters (voltage and feed rate) on the fraction of β-phase and the total crystallinity are represented in Table II. Increasing the applied voltage from 13 to 21 kV in RE samples (spun from pure DMF) demonstrates increase in fraction of β-phase; while, crystallinity calculated in samples spun at feed rate 1 mL/h indicates a significant decrease (10%) with voltage increase.

Electrospun PVDF nanofibers obtained from DMF/acetone mixture (3 : 1) (code TE samples), show an increase in crystallinity when voltage increases from 13 kV to 21 kV. However the fraction of β-phase decreases at 1 mL/h flow rate with increasing the applied voltage (Table III).

In samples containing DMF/acetone (1 : 1) (code SE samples), a higher voltage has no influence on the fraction of β-phase and crystallinity (Table IV).

The effect of applied voltage on the total crystallinity can be attributed to the fact that the electrostatic field may cause the polymer molecules to be more ordered during the electrospinning, thus could induce a greater crystallinity in the formed fibers. However, as there are other parameters that also affect the crystallinity of the fiber, a decrease in crystallinity can be seen in a faster feeding rate (Table II). Upon increasing the voltage, the acceleration of the fibers towards the collector increases which in turn reduces the flight time of the electrospinning jet. There should be a certain time span to allow the polymer molecules to be oriented during the electrospinning. In fact, the reduced flight time means that the fibers are deposited before the polymer molecules have sufficient time to align themselves. Thus, given sufficient flight time, the crystallinity of the fiber will increase with higher voltage.[43] Therefore, it seems that when the evaporation rate of the solvent and the applied flow rate do not provide enough flight time for the polymeric jet,

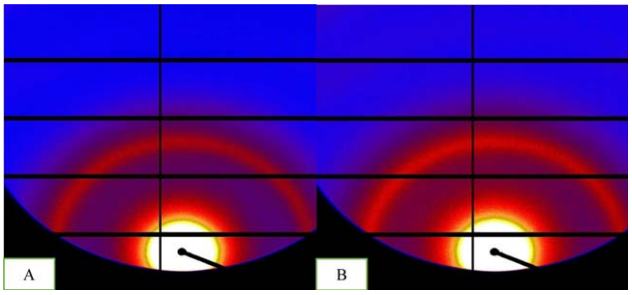

Figure 9. WAXD pattern of electrospun PVDF nanofibers at traveling distance of 17 cm, voltage 13 kV, and flow rate of 0.5 mL/h (code RE-1 and RE-2 samples). [Color figure can be viewed in the online issue, which is available at wileyonlinelibrary.com.]

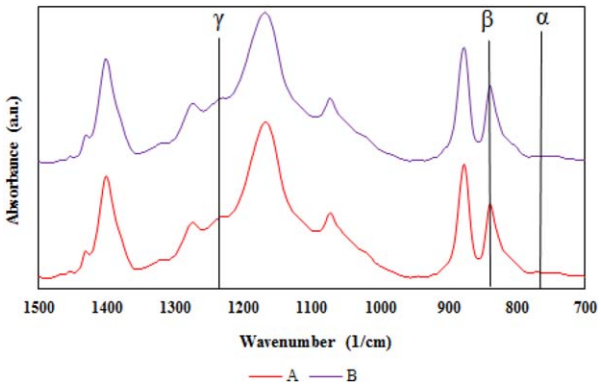

Figure 10. Normalized FTIR spectra of electrospun PVDF nanofibers at traveling distance of 17 cm, voltage 13 kV, and flow rate of (A) 0.5 and (B) 1 mL/h (code RE-1 and RE-2 samples). Curves are shifted vertically for clarity. [Color figure can be viewed in the online issue, which is available at wileyonlinelibrary.com.]

Table V. Fraction of β-Phase $F(\beta)$ of the Electrospun PVDF at the Constant Voltage of 21 kV

Sample	$F(\beta)$ (flow rate = 0.5 mL/h)	$F(\beta)$ (flow rate = 1 mL/h)
RE	0.83	0.82
TE	0.84	0.81
SE	0.83	0.82

Table VI. Total Crystallinity of the Electrospun PVDF Nanofibers at the Constant Voltage of 13 kV

Sample	X_{total} (flow rate = 0.5 mL/h)	X_{total} (flow rate = 1 mL/h)
RE	0.53	0.59
TE	0.41	0.45
SE	0.42	0.47

crystallinity and fraction of β-phase of the resulting nanofibers decreases by increase in voltage.

Influence of Flow Rate

Morphological Properties. The flow rate will determine the amount of solution available for electrospinning. For a given voltage, there is a corresponding flow rate if a stable Taylor cone is to be maintained.[43] The influence of flow rate was investigated while voltage kept constant either at 13 or 21 kV with a needle diameter of 0.75 mm. The fiber diameter increases with increasing the flow rate as shown in Figures 7 and 8.

Due to the greater volume of solution drawn from the needle tip as a result of further amount of flow rate, the jet will take a longer time to dry. As a result, the solvent in the deposited fibers may not have enough time to evaporate given the same flight time. The residual solvents may cause the fibers to fuse together when forming the electrospun webs. A lower flow rate is more desirable as the solvent will have more time for evaporation.[43]

Polymorphism and Crystallinity. The WAXD pattern of the RE samples at different flow rates are shown in Figure 9. The β-phase characteristic arcs ((110), (200) diffraction points) can be clearly seen. FTIR results are shown in Figure 10 and support the WAXD results. According to the FTIR spectra, when the flow rate increases from 0.5 to 1 mL/h, the fraction of β-phase, decreases slightly.

The fraction of β-phase and the total crystallinity calculated from the FTIR and DSC are shown in Tables V and VI. The result reveals that the total crystallinity increases with the flow rate in most samples. For a constant 13 kV voltage and a fixed spinning distance of 17 cm, rising the flow rate leads to increase in total crystallinity from 53% to 59%, according to the calculated data based on the DSC analysis.

Overall, it can be concluded that by increasing the flow rate from 0.5 to 1 mL/h, in most electrospun PVDF nanofibers produced either from pure DMF or DMF/acetone mixture, total crystallinity increases while the fraction of β-phase decreases slightly.

Influence of Solvent

Morphological Properties. SEM images of electrospun PVDF nanofibers obtained from electrospinning of 20% PVDF solutions in pure DMF and DMF/acetone with different volume ratios are shown in Figure 10. Using pure DMF as solvent resulted in

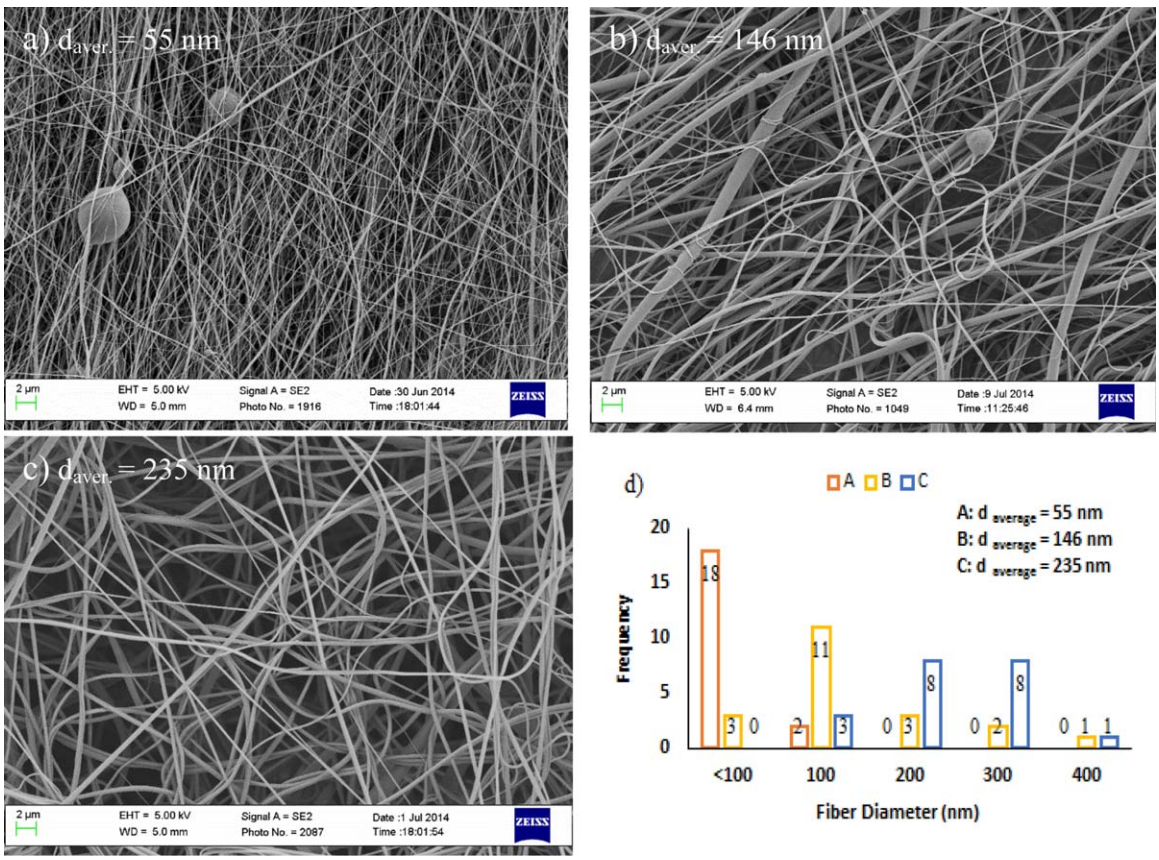

Figure 11. Morphology of electrospun PVDF nanofibers at traveling distance of 17 cm, voltage 13 kV, and flow rate of 0.5 mL/h, with different DMF/acetone ratios (a) DMF (code RE-1), (b) DMF/acetone : 3/1 (code TE-1), (c) DMF/acetone : 1/1 (code SE-1), and (d) diameter distribution of fibers. [Color figure can be viewed in the online issue, which is available at wileyonlinelibrary.com.]

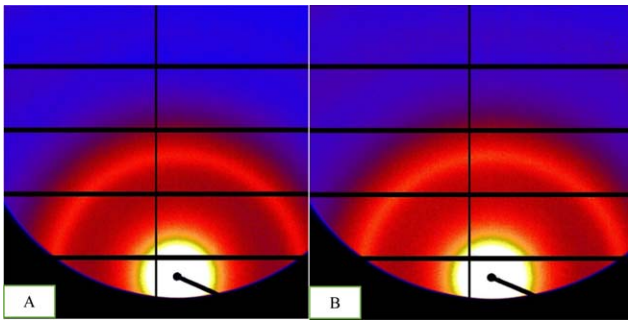

Figure 12. WAXD pattern (A) TE-1 samples and (B) SE-1 samples at traveling distance of 17 cm, flow rate 0.5 mL/h, and voltage of 13 kV. [Color figure can be viewed in the online issue, which is available at wileyonlinelibrary.com.]

formation of beaded nanofibers [Figure 11(a)]. Addition of acetone in solvent mixture (code TE-1 to TE-4 samples), results in less number of beads in electrospun nanofibers [Figure 11(b)] while the fiber diameters substantially increased [Figure 11(d)].

Furthermore, the bead-free ultrafine fibers obtained [Figure 11(c)] when the acetone concentration in the solution increased to 50% (code SE samples). In contrast, fiber diameters increase [Figure 11(d)] when the amount of acetone exceeded 50% in DMF/acetone volume ratio of 1/3 (0.75 acetone). Electro spinning process was stopped as a result of needle block. Uniform ultrafine fibers could be formed when a certain amount of acetone was added into the PVDF polymer solutions. This could be due to the more volatile nature of acetone compared to DMF. Increased amount of acetone led to formation of more uniform fibers.[47]

Polymorphism and Crystallinity. WAXD patterns of TE-1 to TE-4 and SE-1 to SE-4 samples (Figure 12) also show the formation of β polymorph phase. Figure 13 shows the FTIR spectra of the RE-1, SE-1, and TE-1 samples. General features of the FTIR spectra of various samples are similar and samples show the β characteristic peaks i.e. 840 and 1279[44,48] without any sign of γ polymorph, 810 which confirms the WAXD result.

When 25% acetone was added in the electrospinning PVDF solutions (code TE-1 to TE-4), in most samples an increases in

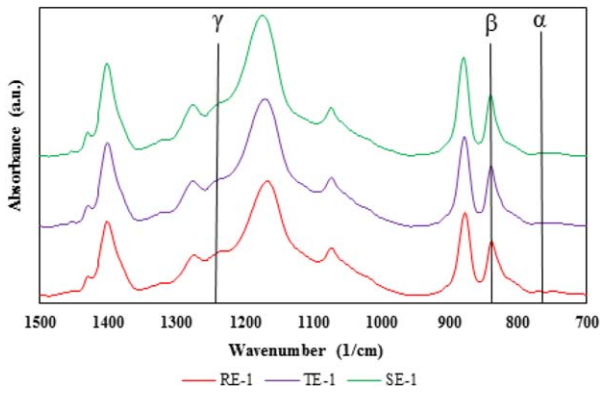

Figure 13. Normalized FTIR spectra of the RE-1, SE-1, and TE-1 samples at traveling distance of 17 cm, flow rate 0.5 mL/h, and voltage of 13 kV. Curves are shifted vertically for clarity. [Color figure can be viewed in the online issue, which is available at wileyonlinelibrary.com.]

Table VII. Fraction of β-Phase $F(\beta)$ and Total Crystallinity of the Electrospun PVDF Nanofibers (Voltage = 13 kV, Flow Rate = 0.5 mL/h)

Sample	$F(\beta)$	X_{total}
RE (DMF)	0.80	0.53
TE (DMF/acetone : 3/1)	0.83	0.41
SE (DMF/acetone : 1/1)	0.84	0.42

fraction of β-phase is observed compared with samples spun from pure DMF (code RE-1 to RE-4); while there is a significant decrease (up to 14%) in the total crystallinity of all samples. Table VII shows the influence of adding acetone into the electrospinning solutions.

Addition of 50% acetone to DMF in the electrospinning PVDF solutions (code SE-1 to SE-4) increased the $F(\beta)$ but decreased the X_{total}. It can be interpreted that fast evaporation of the solvent has solidified the fiber; therefore, macromolecular alignment during stretching have immobilized which results high fraction of the β polymorph. Thus, combining low evaporation rate DMF with high evaporation rate acetone gives us the ability to adjust the solvent evaporation rate and consequently adjust the polymorphism.

However increasing the acetone led to an increase in the total crystallinity of the electrospun fibers at 13 kV voltage. Nevertheless, the total crystallinity reduced for electrospun nanofibers at 21 kV, as shown in Table VIII.

The results are inconsistent with what has been reported in the literature[43] indicating that higher voltage can induce a higher crystallinity in the fiber up to the a certain point, at which the crystallinity of the fiber reduces.

Ultrafine fibers with diameters lower than 100 nm were obtained in this work. As discussed earlier, fiber diameters decrease with increasing the voltage (from 13 to 21 kV). On the other hand, increasing the flow rate (from 0.5 to 1 mL/h) as well as adding acetone to DMF in the electrospinning solutions results in increased fiber diameter. The minimum fiber diameter of 12–32 nm was obtained from the solution in which pure DMF was used as solvent at voltage of 21 kV and flow rate of 0.5 mL/h (code RE-3) (Figure 14).

CONCLUSION

In the present work, PVDF was electrospun from 20% w/w polymer solution in DMF and DMF/acetone with volume ratios of 3/1 and 1/1. In case of DMF/acetone volume ratio of 1/3, the spinning process was stopped as a result of needle block. The influence of processing and solution parameters such as flow rate, applied voltage, solvents type, and mixture ratio, on nanofiber

Table VIII. Total Crystallinity of the Electrospun PVDF Nanofibers at Flow Rate of 0.5 mL/h

Sample	X_{total} voltage = 13 kV	X_{total} voltage = 21 kV
TE (DMF/acetone : 3/1)	0.41	0.49
SE (DMF/acetone : 1/1)	0.42	0.42

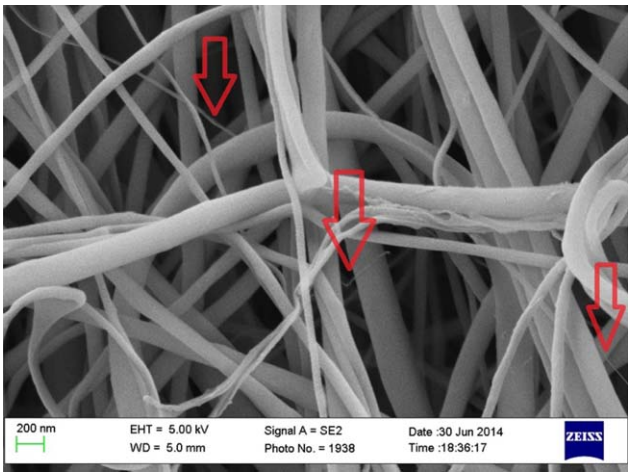

Figure 14. SEM image of ultrafine PVDF polymer nanofibers (code RE-3), the ultrafine fibers are marked with the arrows. The diameters are 32, 15, and 12 nm from left to right. [Color figure can be viewed in the online issue, which is available at wileyonlinelibrary.com.]

morphology, total crystallinity, and crystal phase content of PVDF fibers were studied. The diameter of the PVDF electrospun fibers decreased gradually with increasing the applied voltage. The obtained fraction of β-phase in current work was in the range of 79%–85%. Decreasing the flow rate and giving sufficient flight time to the polymer jet, resulted in raising the crystallinity of the fibers with higher voltages. Uniform ultrafine fibers were formed when a certain amount of acetone was added into the electrospun PVDF solution. By increasing the flow rate from 0.5 to 1 mL/h, in most samples, total crystallinity increases. Adding 25% acetone into the electrospinning PVDF solution, a significant decrease (up to 14%) in total crystallinity of samples was observed. The range of applied voltages and flow rates used in the present study did not show a significant influence on the electroactive β-phase content. However adding 25% acetone in the electrospun PVDF solution, led to an increase in fraction of β-phase (up to 5%) compared to samples spun from pure DMF.

The 2D-WAXD measurements were carried out at the Australian Synchrotron, Victoria, Australia. The authors thank Dr. Nigel Kirby and Tao Zhang for the 2D-WAXD measurements. The corresponding author also thanks financial support from the Iran National Science Foundation (INSF) and anonymous reviewers for their stimulating suggestions and remarks.

REFERENCES

1. Tõnurist, K.; Thomberg, T.; Jänes, A.; Romann, T.; Sammelselg, V.; Lust, E. *ECS Transactions* **2013**, *50*, 49.
2. Baji, A.; Mai, Y.-W.; Li, Q.; Liu, Y. *Compos. Sci. Technol.* **2011**, *71*, 1435.
3. Chinnappan, A.; Kim, H. *Int. J. Hydrogen Energy* **2012**, *37*, 18851.
4. Abolhasani, M.; Jalali-Arani, A.; Nazockdast, H.; Guo, Q. *Polymer* **2013**, *54*, 4686.
5. Abolhasani, M. M.; Guo, Q.; Jalali-Arani, A.; Nazockdast, H. *J. Appl. Polym. Sci.* **2013**, *130*, 1247.
6. Abolhasani, M. M.; Naebe, M.; Jalali-Arani, A.; Guo, Q. *NANO* **2014**, *9*, 1450065.
7. Abolhasani, M. M.; Naebe, M.; Guo, Q. *Phys. Chem. Chem. Phys.* **2014**, *16*, 10679.
8. Abolhasani, M. M.; Abadchi, M. R.; Magniez, K.; Guo, Q. *J. Therm. Anal. Calorim.* **2015**, *119*, 527.
9. Persano, L.; Dagdeviren, C.; Su, Y.; Zhang, Y.; Girardo, S.; Pisignano, D.; Huang, Y.; Rogers, J. A. *Nat. Commun.* **2013**, *4*, 1633.
10. Rahman, A.; Chung, G.-S. *J. Alloys Compd.* **2013**, *581*, 724.
11. Abolhasani, M. M.; Zarejousheghani, F.; Cheng, Z.; Naebe, M. *RSC Adv.* **2015**, *5*, 22471.
12. Ahn, Y.; Lim, J. Y.; Hong, S. M.; Lee, J.; Ha, J.; Choi, H. J.; Seo, Y. J. *J. Phys. Chem. C* **2013**, *117*, 11791.
13. Tang, C.-W.; Li, B.; Sun, L.; Lively, B.; Zhong, W.-H. *Eur. Polym. J.* **2012**, *48*, 1062.
14. Yu, S.; Zheng, W.; Yu, W.; Zhang, Y.; Jiang, Q.; Zhao, Z. *Macromolecules* **2009**, *42*, 8870.
15. Luo, H.; Huang, Y.; Wang, D. *Polymer* **2013**, *54*, 4710.
16. Fashandi, H.; Yegane, A.; Abolhasani, M. M. *Fiber Polym.* **2015**, *16*, 326.
17. Ribeiro, C.; Sencadas, V.; Ribelles, J. L. G.; Lanceros-Méndez, S. *Soft Matter* **2010**, *8*, 274.
18. Liu, Z.; Pan, C.; Lin, L.; Lai, H. *Sens. Actuators A* **2013**, *193*, 13.
19. Chang, J.; Dommer, M.; Chang, C.; Lin, L. *Nano Energy* **2012**, *1*, 356.
20. Xing, C.; Guan, J.; Li, Y.; Li, J. *ACS Appl. Mater. Inter.* **2014**, *6*, 4447.
21. Liao, Y.; Wang, R.; Tian, M.; Qiu, C.; Fane, A. G. *J. Membr. Sci.* **2013**, *425*, 30.
22. Nakashima, R.; Watanabe, K.; Lee, Y.; Kim, B. S.; Kim, I. S. *Adv. Polym. Technol.* **2011**, *32*, E44.
23. Yee, W. A.; Nguyen, A. C.; Lee, P. S.; Kotaki, M.; Liu, Y.; Tan, B. T.; Mhaisalkar, S.; Lu, X. *Polymer* **2008**, *49*, 4196.
24. Naebe, M.; Lin, T.; Staiger, M. P.; Dai, L.; Wang, X. *Nanotechnology* **2008**, *19*, 305702.
25. Naebe, M.; Lin, T.; Staiger, M.; Dai, L.; Wang, X. *Nanotechnology* **2008**, *19*, 8.
26. Neppalli, R.; Wanjale, S.; Birajdar, M.; Causin, V. *Eur. Polym. J.* **2013**, *49*, 90.
27. Chanunpanich, N.; Lee, B.; Byun, H. *Macromol. Res.* **2008**, *16*, 212.
28. Zare, Y. *Synthetic Met.* **2015**, *202*, 68.
29. Huang, Z.-M.; Zhang, Y.-Z.; Kotaki, M.; Ramakrishna, S. *Compos. Sci. Technol.* **2003**, *63*, 2223.
30. Khajavi, R.; Abbasipour, M. *Scientia Iranica* **2012**, *19*, 2029.
31. Wang, X.; Ding, B.; Sun, G.; Wang, M.; Yu, J. *Progr. Mater. Sci.* **2013**, *58*, 1173.
32. Ma, X.; Liu, J.; Ni, C.; Martin, D. C.; Chase, D. B.; Rabolt, J. F. *ACS Macro Lett.* **2012**, *1*, 428.
33. Naebe, M.; Lin, T.; Wang, X. Carbon Nanotubes Reinforced Electrospun Polymer Nanofibers [online]. In: Nanofibers;

Kumar, A., Ed.; **2010**; Chapter 16, pp 309–328. DOI: 10.5772/8160. Available at: http://www.intechopen.com/books/nanofibers/carbon-nanotubesreinforcedelectrospun-polymer-nanofibres. Accessed on February 1, 2010.

34. Naebe, M.; Tong, L.; Lianfang, F.; Liming, D.; Abramson, A.; Prakash, V.; Xungia, W. Conducting polymer and polymer/CNT composite nanofibers by electrospinning. In ACS Symposium Series; Oxford University Press; **2009**, Vol. 1016, pp 39–58.
35. Heidari, I.; Mosavi Mashhadi, M.; Faraji, G. *Chem. Phys. Lett.* **2013**, *590*, 231.
36. Gupta, P.; Wilkes, G. L. *Polymer* **2003**, *44*, 6353.
37. Lei, T.; Cai, X.; Wang, X.; Yu, L.; Hu, X.; Zheng, G.; Lv, W.; Wang, L.; Wu, D.; Sun, D. *RSC Adv.* **2013**, *3*, 24952.
38. Zhang, P.; Zhao, X.; Zhang, X.; Lai, Y.; Wang, X.; Li, J.; Wei, G.; Su, Z. *ACS Appl. Mater. Inter.* **2014**, *6*, 7563.
39. Cozza, E. S.; Monticelli, O.; Marsano, E.; Cebe, P. *Polym. Int.* **2013**, *62*, 41.
40. Liu, Y.-L.; Li, Y.; Xu, J.-T.; Fan, Z.-Q. *Appl. Mater. Inter.* **2010**, *2*, 1759.
41. Zheng, J.; He, A.; Li, J.; Han, C. C. Macromol. *Macromol. Rapid Commun.* **2007**, *28*, 2159.
42. Yee, W. A.; Kotaki, M.; Liu, Y.; Lu, X. *Polymer* **2007**, *48*, 512.
43. Ramakrishna, S.; Fujihara, K.; Teo, W.-E.; Lim, T.-C.; Ma, Z. Electrospinning Process. In: An introduction to electrospinning and nanofibers; World Scientific, **2005**; Vol. 90, p 105.
44. Martins, P.; Lopes, A.; Lanceros-Mendez, S. *Prog. Polym. Sci.* **2013**, *39*, 683.
45. Andrew, J.; Clarke, D. *Langmuir* **2008**, *24*, 670.
46. Benz, M.; Euler, W. B. *J. Appl. Polym. Sci.* **2003**, *89*, 1093.
47. Zhao, Z.; Li, J.; Yuan, X.; Li, X.; Zhang, Y.; Sheng, J. *J. Appl. Polym. Sci.* **2005**, *97*, 466.
48. Abolhasani, M. M.; Naebe, M.; Jalali-Arani, A.; Guo, Q. *PLoS One* **2014**, *9*, e88715.

SGML and CITI Use Only
DO NOT PRINT